Journal of Colloid and Interface Science 557 (2019) 628–634

Contents lists available at ScienceDirect

Journal of Colloid and Interface Science

journal homepage: www.elsevier.com/locate/jcis

Assembled cationic dipeptide-gold nanoparticle hybrid microspheres for electrochemical biosensors with enhanced sensitivity

Keqing Wang [a,b], Ziruo Li [a,c], Chenlei Wang [a,b], Shuo Zhang [c], Wei Cui [a], Youqian Xu [a], Jie Zhao [a], Huimin Xue [a,b], Junbai Li [a,b,*]

[a] Beijing National Laboratory for Molecular Sciences (BNLMS), CAS Key Laboratory of Colloid, Interface and Chemical Thermodynamics, Institute of Chemistry, Chinese Academy of Sciences, Beijing 100190, China
[b] University of Chinese Academy of Sciences, Beijing 100049, China
[c] CAS Key Laboratory for Biomedical Effects of Nanomaterials and Nanosafety, National Center for Nanoscience and Technology, Beijing 100190, China

GRAPHICAL ABSTRACT

Schematic process of assembling CDP-AuNP hybrid microspheres and fabrication of ChOx/CDP-AuNP/CS/PB biosensor electrodes.

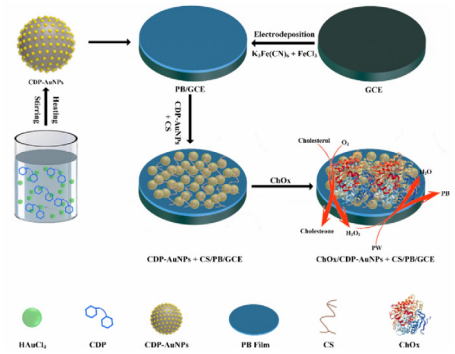

GCE: glassy carbon electrode
CDP: cationic dipeptide
CDP-AuNPs: cationic dipeptide-gold nanoparticles
ChOx: cholesterol oxidase
$HAuCl_4$: chloroauric acid
CS: chitosan
PB : Prussian blue
PW: Prussian white

ARTICLE INFO

Article history:
Received 28 July 2019
Revised 8 September 2019
Accepted 10 September 2019
Available online 11 September 2019

Keywords:
Cationic dipeptide
AuNPs
Molecular assembly
Cholesterol
Electrochemical biosensor

ABSTRACT

Molecular assemblies of cationic dipeptide-gold nanoparticle (CDP-AuNP) hybrid microspheres were used to modify cholesterol oxidase electrodes for high-sensitivity cholesterol detection. The cationic dipeptide used here serves as a functional molecule for adsorbing chloroauric acid based on electrostatic interactions and assembly into spherical structures, providing a platform for loading gold nanoparticles (AuNPs), increasing the immobilization load of the enzyme and maintaining the activity of the enzyme as a result of excellent biocompatibility. Moreover, the CDP-AuNP modified cholesterol oxidase electrode has a higher electrocatalytic activity to cholesterol with obvious enhancement in the current response, exhibiting a current response 13 times higher than that of the controlled electrode. The outstanding biocompatibility and increased enzyme load by hybrid microspheres and the good charge-transfer ability of AuNPs in the peptide-based electrode indicate a very attractive perspective in the field of biodevices.

* Corresponding author.
E-mail address: jbli@iccas.ac.cn (J. Li).

https://doi.org/10.1016/j.jcis.2019.09.033
0021-9797/

1. Introduction

Micro-/nanostructures fabricated from biological building blocks have promising prospects for biology and nanotechnology applications [1–3]. The diphenylalanine molecule, as one of bioactive peptides, is the simplest block for constructing biological micro-/nanostructure materials, as it has the advantages of biocompatibility, simple chemical modification or biological function, and easy synthesis and manipulation [4–6]. The cationic dipeptide (CDP), C-terminal amidated diphenylalanine, possesses the advantage of a positive charge, providing additional applications. Diphenylalanine and its derivative-based nanomaterials with various structures have been constructed through a controlled processes [7–13] and exhibit excellently optical, mechanical and electrochemical properties [14–20]. Gazit and coworkers first used peptide-based nanotube-modified electrodes for electrochemical biosensing detection with improved sensitivity [21]. Subsequently, a series of peptide-based nanomaterials have been demonstrated in biosensors with enhanced electrochemical properties [22–24]. Very recently, Yang and coworkers presented a nice work on diphenylalanine-gold nanoparticle hybrid spheres for highly sensitive hydrogen peroxide (H_2O_2) detection [25]. The combination of dipeptide and metal nanoparticles with primary conductivity is a much better choice to remarkably enhance the sensitivity of the devices [25,26].

Cholesterol is not only an essential component of nerve tissues, brain cells, plasma membranes, and liver but also an important precursor of hormones, vitamin D, etc. [27]. As abnormal levels of cholesterol in blood may lead to clinical disorders, the accurate detection of cholesterol has increasingly received attention for improving human health [28,29]. Several analytical methods have been previously reported to detect cholesterol, such as spectrophotometry, gas–liquid chromatography, and colorimetric methods [30,31], which are sophisticated procedures that require time or lack sensitivity. Thus, electrochemical cholesterol biosensors have captured researchers' attention due to their low cost, good portability, high sensitivity, and rapid and accurate quantification. However, the reduction of H_2O_2 occurs at a more negative potential than −1.0 V. A thin Prussian blue film cast on the surface of the electrode prior to cholesterol oxidase (ChOx) immobilization can provide better sensitivity and more positive potential for H_2O_2 detection to avoid interferences from some electroactive species [32]. Moreover, immobilization of ChOx onto the matrix is also a pivotal step for cholesterol enzyme biosensors. Whereas, challenges remain to be addressed. The development of a primary matrix that can maintain enzyme activity, increase enzyme load and enhance the sensitivity of the biosensors is also an intensive requirement [33]. The biomaterials constructed from the cationic dipeptide and gold nanoparticles, namely, cationic dipeptide-gold nanoparticle (CDP-AuNP) hybrid microspheres, will provide a better matrix for this purpose.

Herein, the prepared CDP-AuNP hybrid microspheres serve as a modifier, which can improve the electroconductivity of the assembly and enhance the catalytic activity owing to the embedded gold nanoparticles. It also increases the immobilization load of ChOx on the PB-based film due to its biocompatibility. The obtained hybrid microspheres were further used to modify cholesterol oxidase (ChOx) electrodes to form electrochemical cholesterol biosensors with significantly improved sensitivity. The prepared dipeptide-based composites inherited the advantages of dipeptide and gold nanoparticles. Thus, the constructed electrochemical enzyme sensors can realize highly effective detection of cholesterol with high selectivity, excellent sensitivity, a wide linear range and a low detection limit. The results indicate that the assembled microsphere may also be potentially used for fabricating other highly sensitive and stable electrochemical biodevice.

2. Experimental section

2.1. Reagents and materials

Cholesterol oxidase (ChOx) ((EC 1.1.3.6, 50 U/mg), chitosan (CS) and Triton-X 100 (polyoxyethylene isooctylphenyl ether) were purchased from Sigma (Shanghai, China). 1,1,1,3,3,3-Hexafluoro-2-propanol (HFIP), cholesterol (95%), ascorbic acid (AA), glycine, dopamine (DA), glucose and glutaraldehyde were obtained from Sigma-Aldrich. Cationic dipeptide (CDP, H-Phe-Phe-NH_2·HCl) was obtained from Bachem (Bubendorf, Switzerland). Serum samples were obtained from Reanta. Chloroauric acid ($HAuCl_4$) and other chemicals were purchased from the Beijing Chemical Reagent Company (Beijing, China). All reagents were used without further purification. All solutions were prepared with ultrapure water from a Milli-Q purification system (18.2 MΩ, Milli-Pore, Bedford, MA, USA).

2.2. Instrument and measurements

Scanning electron microscopy (SEM) images were recorded with an S-4800 (HITACHI, Japan) equipped with energy-dispersive X-ray spectroscopy (EDS). Transmission electron microscopy (TEM) images were obtained on an HT-7700. A suspension of CDP-AuNP hybrid microspheres was dropped onto a silicon wafer and a copper grid and dried at room temperature for SEM and TEM detection. The absorption spectra were obtained by using a UV–vis 3100 spectrometer. Dynamic light scattering (DLS) data were obtained by a Zetasizer Nano ZS (ZEN3600, Malvern Instruments Ltd., UK). Fourier transform infrared (FT-IR) spectroscopy of CDP and CDP-AuNP was performed by TENSOR-27 (BRUKER, Germany). All electrochemical experiments were carried out on a CHI 660E electrochemical workstation (Beijing, China) with a three-electrode system consisting of a bare or modified glassy carbon electrode as the working electrode, a platinum wire as the counter electrode, and an Ag/AgCl electrode as the reference electrode.

2.3. Preparation of CDP-AuNP microspheres and nanospheres

Some modifications were used to prepare the hybrid microspheres [25]. First, 4 mg of CDP was dissolved in 40 μL of HFIP solution. Then, 40 μL of CDP solution was mixed with 2 mL of $HAuCl_4$ (0.5 mM) solution. The mixed solution was stirred for 30 min, followed by heat treatment at 60 °C in the dark for 2 h. The CDP-AuNP hybrid microspheres could be obtained in steps. As previously reported, glutaraldehyde solution can better control the size of the assembled cationic dipeptides to form nanospheres [34]. For the preparation of hybrid nanospheres, there is a further modification. Before adding 40 μL of CDP solution into the $HAuCl_4$ solution, 40 μL of glutaraldehyde solution (6%) was added to CDP solution, followed by mixing with the $HAuCl_4$ solution.

2.4. Preparation of cholesterol solution

Isopropanol and Triton-X 100 are effective solubilizing agents for cholesterol. Therefore, cholesterol stock solution with a concentration of 10 mM was well prepared as follows. 203.5 mg cholesterol was dissolved in a mixture of 5 mL isopropanol and 5 mL Triton-X 100 and then diluted with 40 mL ultrapure water in a bath at 60 °C. The serum was diluted with a phosphate buffer solution (PBS, pH 7.0) containing Triton-X 100 (1% (m/v)) and isopropanol (2% (v/v)).

2.5. Preparation of a cholesterol sensor

Prior to use, a glassy carbon electrode (GCE, diameter 3 mm) was mechanically polished with 1.0, 0.3, and 0.05 μm alumina slurry to form a mirror-like surface, followed by rinsing with doubly distilled water and drying by nitrogen. A Prussian blue mediator layer was electrodeposited onto the GCE by +0.4 V for 60 s in a fresh solution containing 5 mM $FeCl_3$, 100 mM KCl, 5 mM $K_3Fe(CN)_6$, and 100 mM HCl. After deposition, the PB modified electrode was electrochemically activated in 0.1 M HCl-KCl (pH 7.0). The treated electrode was washed and dried at room temperature for 30 min. All electrochemical experiments were carried out at approximately 25 °C.

The enzyme electrode was fabricated by a simple casting method as follows. First, chitosan (CS) was dissolved in 2% acetic acid and stirred for 1 h. Next, 3 μL of CS solution was mixed with 2 μL of CDP-AuNP microspheres (2 mg/mL). The mixture was drop onto a PB/GC electrode to form CDP-AuNPs/CS/PB/GCE, followed by drying at room temperature and washing with water. To prepare the cholesterol sensors, 10 μL of ChOx (10 mg ml^{-1} in PBS at pH 7.0) was dropped onto the surface of CDP-AuNPs/CS/PB/GCE to fabricate a ChOx/CDP-AuNPs/CS/PB/GCE biosensor. Finally, the modified electrodes were washed thoroughly with doubly distilled water to remove unbound enzymes. In a controlled experiment, a ChOx/CS/PB/GCE biosensor with CDP-AuNP nanospheres or without CDP-AuNP microspheres was fabricated using the same procedure.

3. Results and discussion

3.1. Preparation and morphological characterization of CDP-AuNP hybrid spheres

The strategy used to prepare the CDP-AuNP hybrid microspheres and CDP-AuNP-based biosensors is displayed in Fig. 1. First, the CDP/HFIP solution was mixed with the $HAuCl_4$ solution. After heat treatment for 2 h at 60 °C, the color of the mixture changed to light purple, indicating that the Au^{3+} was reduced to gold nanoparticles and further formed CDP-AuNP hybrid microspheres. A previous study demonstrated that the dipeptide can act as a reductant for gold ions to form AuNPs without adding any reducing agent [25,35]. This formation can also be proved by the UV–vis adsorption spectra in Fig. S1. The CDP-AuNP hybrid microspheres illustrated an adsorption peak for AuNPs at 525 nm.

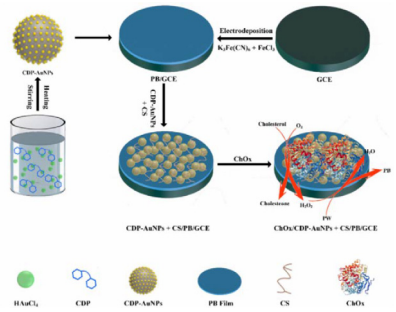

GCE: glassy carbon electrode
$HAuCl_4$: chloroauric acid
CDP: cationic dipeptide
CS: chitosan
CDP-AuNPs: cationic dipeptide-gold nanoparticles
PB: Prussian blue
ChOx: cholesterol oxidase
PW: Prussian white

Fig. 1. Schematic process of assembling CDP-AuNP hybrid microspheres and fabrication of ChOx/CDP-AuNP/CS/PB biosensor electrodes.

According to the method mentioned above, we prepared hybrid microspheres and nanospheres. Then, the obtained hybrid microspheres and nanospheres were characterized by SEM, EDS and DLS, as shown in Fig. 2. The typical SEM images in Fig. 2A and C and the TEM image in Fig. 2B also demonstrate the 1.5 μm diameters of the microspheres, whereas 300 nm diameters of the nanospheres are observed in Fig. 2E and F. Both spherical structures were well embedded with AuNPs on their surfaces. Obviously, the Au element mapping analysis results confirmed that the AuNPs were on the surface of the microspheres (Fig. 2D). In the dynamic light scattering (DLS) data (Fig. S2), the diameter ranged from 0.8 to 1.8 μm for microspheres and from 300 to 500 nm for nanospheres, which agreed well with the SEM images and TEM images. In addition to the different sizes between the two spheres, the hybrid microsphere might load more AuNPs than the hybrid nanosphere due to its larger surface area.

3.2. Structure characterization of CDP-AuNP microspheres

According to the previous assembly mechanism of the CDP [16], diphenylalanine [36,37], and the other peptide-AuNP hybrids [38,39], a possible formation mechanism of the CDP-AuNP hybrid microspheres was proposed as follows. The CDP can self-assemble into nanotubes at physiological pH values and further rearrange to form vesicles upon dilution [16]. Intriguingly, gold ions not only introduced gold particles, resulting in hybrid dipeptide composites, but also affected the assembly process of the dipeptide and eventually determined its morphology and structures [25]. The cationic dipeptide served as a functional molecule, making equal contributions to the preparation of hybrid microspheres. The low concentrations of CDP and $AuCl_4^-$ can contribute to the formation of CDP-AuNP hybrid microspheres. The electrostatic interaction between positive CDP and negative $AuCl_4^-$ also makes the assembly process much easier and the microsphere more stable.

To investigate the molecular interactions and structures during the assembly process, CDP (red lines) and CDP-AuNP (blue lines) were characterized by FTIR, as shown in Fig. 3. The C═O bond stretching vibration appeared at 1666 cm^{-1} in CDP and shifted to 1668 cm^{-1} in CDP-AuNP, which suggested that the conjugation of carbonyl bonds is achieved via the electronegative interaction with carbonyl oxygen. The peak at 1330 cm^{-1} was attributed to the C—N vibration of the aromatic amine. The bending N—H vibration and stretching N—H vibration in CDP-AuNP were observed at approximately 1495 and 3202 cm^{-1}, respectively, which were slightly blue-shifted compared with those of CDP (1475 and 3170 cm^{-1}, respectively). The shift confirmed the interactions between the dipeptide and AuNPs, which were realized via the *N*-terminal peptide amino group [25]. The obtained hybrid microsphere, as an immobilized matrix of ChOx, could be further used for electrochemical biosensors.

3.3. Electrochemical characterization of the modified GCE

Cholesterol oxidase (ChOx) is commonly used to fabricate cholesterol enzyme biosensing and catalytic cholesterol to H_2O_2. However, the reduction of H_2O_2 appears at a more negative potential than −1.0 V. A thin Prussian blue film cast on the surface of the electrode prior to ChOx immobilization can provide more positive potential for H_2O_2 detection to avoid interferences. Hence, an electrochemical biosensor for cholesterol detection was constructed as follows. First, a Prussian blue (PB) film was electrodeposited on the GCE because electrodeposition often resulted in a PB film with higher catalytic activity, and a thin PB film also has a high sensitivity to H_2O_2. The well-prepared PB film is characterized in detail in Fig. S3 and can decrease the reduction potential of H_2O_2. Cyclic

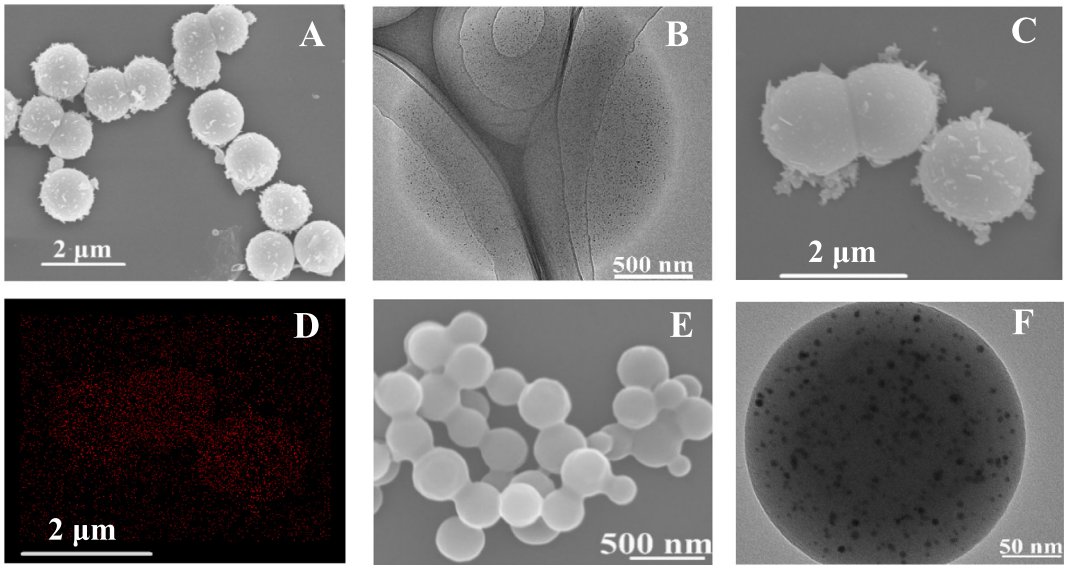

Fig. 2. (A) SEM image and (B) TEM image of CDP-AuNP microspheres, (C) SEM image and (D) Au mapping analysis of CDP-AuNP microspheres, (E) SEM and (F) TEM images of CDP-AuNP nanospheres.

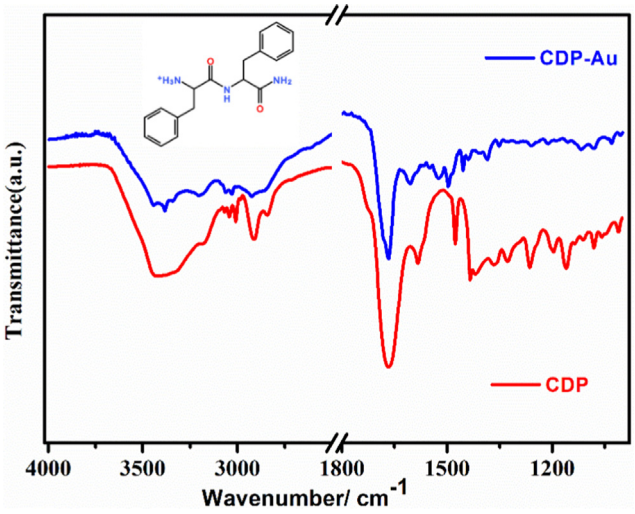

Fig. 3. FTIR spectra of CDP before (CDP, red line) and after hybrid with AuNP (CDP-AuNP) microsphere (blue line). The inset picture is the structural formula of CDP. (For interpretation of the references to colour in this figure legend, the reader is referred to the web version of this article.)

voltammograms (CVs) of bare PB/GCE and different modified PB/GCE were obtained, as shown in Fig. 4A. No obvious signal appeared at GCE (Fig. 4A, curve a). After electrodeposition with the PB layer, the CV of PB/GCE showed a pair of redox peaks, revealing the reduction of Prussian white and the oxidation of PB, respectively (Fig. 4A, curve b). When the ChOx + CDP-AuNP were cast onto the PB film (Fig. 4A, curve c), and both the cathodic and anodic peak currents decreased compared with that of PB/GCE. This result indicated that ChOx + CDP-AuNP could hinder the electron transfer and reduce the reversibility of PB film.

The value of the electron transfer resistance (Ret) can be directly estimated from the diameters of the high frequency semicircle, showing the dielectric and insulating features at the interface of the electrolyte/electrode. $[Fe(CN)_6]^{3-/4-}$ redox couples serve as the electrochemical probe, and the electrochemical impedance spectroscopy (EIS) data of the bare GCE, PB/GCE and ChOx + CDP-AuNP/PB/GCE are shown in Fig. 4B. A typical EIS spectrum of a bare electrode (Fig. 4B, curve a) consisted of a small semicircle (Ret: 150 Ω) and a straight tail line, which corresponded to the features of electron transfer and diffusion processes, respectively. When the GCE electrode surface was coated by a PB film, the Ret increased to approximately 450 Ω (Fig. 4B, curve b). This indicated that the electrodeposited PB film blocked the electron transfer from the electrochemical probe to the electrode. Furthermore, after modifying the ChOx + CDP-AuNP matrix onto CS/PB/GCE (Fig. 4C, curve c), the Ret was much larger than that for other modified electrodes, with a value of approximately 1500 Ω, which may be due to the poor conductivity of the covalently attached ChOx and may block the electron transfer from $K_3Fe(CN)_6$ to the electrode. The results also illustrated that ChOx + CDP-AuNP were successfully immobilized on the PB surface and consistent with the CV experiments.

3.4. Electrochemical characterization of a cholesterol biosensor

The enzymatic reactions for the detection of cholesterol can be realized by indirect detection of oxidizable products of hydrogen peroxide. Sensitively and selectively monitoring H_2O_2 has been previously reported based on detecting the reduction current [40,41] rather than the oxidation current to avoid oxidizable interferents present in real samples at positive potentials [42,43]. The remarkably large positive shift in the potential from −1.0 V for H_2O_2 reduction is obvious, indicating the good electrocatalytic activity of PB to H_2O_2 reduction [32]. Hence, we preferred to use the reduction current of H_2O_2 at 0 V (vs. Ag/AgCl) for detection of cholesterol by the ChOx + CDP-AuNP + CS/PB/GCE biosensor in this study. Immobilized ChOx can act as the first electrocatalyst for cholesterol into H_2O_2, and the PB layer acts as the second electrocatalyst for H_2O_2 into H_2O.

Fig. 5 shows CVs obtained at the various modification stages of PB/GCE in the presence of 1 mM cholesterol. After modification of CDP-AuNPs on the surface of CS/PB/GCE, an oxidation peak current of 10 μA was observed (Fig. 5, curve a), which was due to the good conductivity of AuNPs. The ChOx-modified enzyme electrode also has a larger oxidation peak current than that of CDP-AuNPs/CS/PB/GCE. The redox current increased obviously, and the oxidation current increased to 50 μA (Fig. 5, curve b). Furthermore, CDP-AuNPs and ChOx comodified electrodes were used for

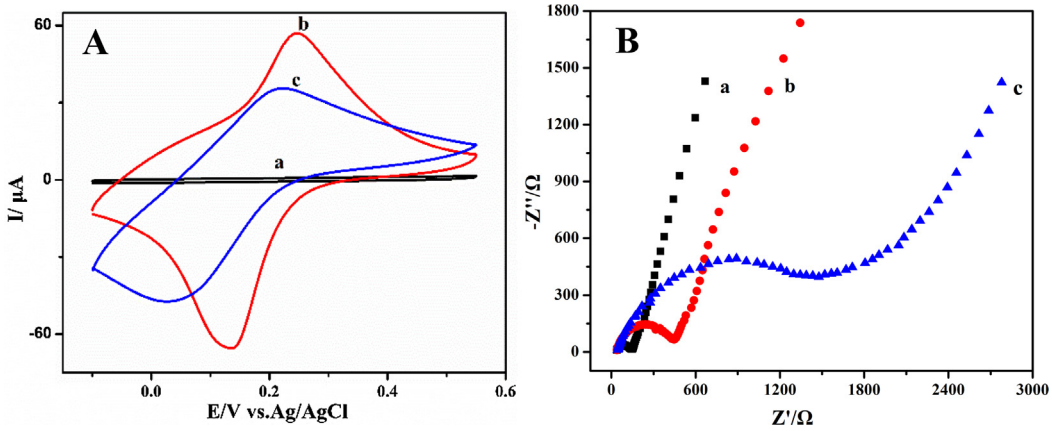

Fig. 4. (A) Cyclic voltammograms at pH 7.0 PBS at (a) GCE, (b) PB/GCE, (c) ChOx + CDP-AuNP + CS/PB/GCE. (B) Nyquist plots obtained at bare GCE, PB/GCE and ChOx + CDP-AuNP + CS/PB/GCE in 5 mM $[Fe(CN)_6]^{3-/4-}$ (1:1).

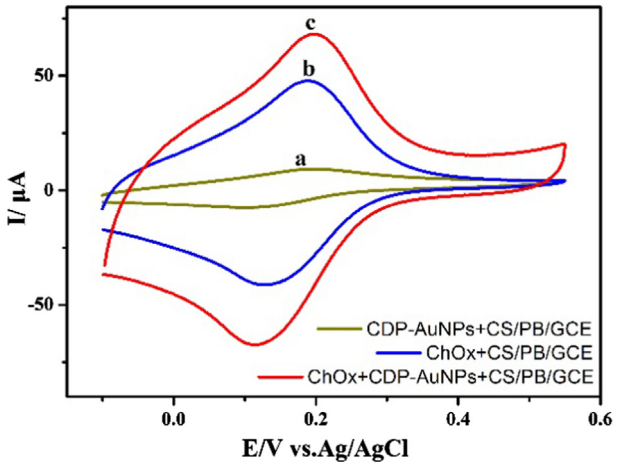

Fig. 5. Cyclic voltammograms obtained at different modified GCEs (CDP-AuNPs, ChOx, CDP-AuNPs + ChOx) in 1 mM cholesterol (pH 7.0 PBS) under ambient air.

electrochemical detection. The higher oxidation peak current (70 μA) obtained from ChOx/CDP-AuNPs/CS/PB/GCE was due to the good conductivity of AuNPs (Fig. 5, curve c) and the biocompatible CDP-AuNP hybrid microspheres, which can increase the immobilization ChOx on the PB-based film electrode. The cholesterol decomposed and produced H_2O_2. We analyzed the enzyme coverage based on previous reports and found that this coverage was higher than the monolayer coverage [44]. According to the Laviron equation, the charge transfer coefficient α and the electron-transfer rate constant (ks) of cholesterol are much larger than those in previous reports, implying a faster electron transfer process, which may be attributed to the nanostructured AuNPs (Fig. S4).

3.5. Quantitative analysis of cholesterol

Fig. 6 depicts the amperometric response of ChOx + CDP-AuNP + CS/PB/GCE and ChOx/CS/PB/GCE (as the controlled electrode) on successive addition cholesterol into PBS (pH 7.0). After adding cholesterol into solution, the current on the CDP-AuNP-based enzyme electrode increased. Catalytic currents displayed a wider linear response from 200 μM to 3.1 mM (Ip (μA) = 0.0956 $C_{cholesterol}$/mM + 0.00027, R^2 = 0.9990) with a detection limit of 50 μM (S/N = 3) than other dipeptide-AuNP microsphere-based sensors [25]. The controlled electrode has a lower current response toward cholesterol under the same conditions. The current response of the ChOx + CDP-AuNP + CS/PB/GCE to the addition of cholesterol at +0 V vs. Ag/AgCl was 13 times higher than that of the enzyme electrode without microsphere modification (ChOx/CS/PB/GCE) at the same potential. Hybrid CDP-AuNP nanospheres were also used to modify the enzyme electrode for cholesterol detection, resulting in a lower response than the CDP-AuNP hybrid microsphere-modified electrode (Fig. S5). Moreover, CDP-AuNP hybrid microspheres embedded with more AuNPs also have a better catalytic effect than CDP-AuNP nanospheres. The nanostructured AuNPs in the hybrid microsphere modified enzyme electrode act as good electron acceptors and transfer them to the underlying PB/GCE, leading to improved electrocatalysis and higher k_s values [45]. The gold nanoparticles have high affinity for molecules containing thiol/amine groups, providing a much easier platform for electrode surface modification [46]. Further, the hybrid microspheres possess a high surface-to-volume ratio for the immobilization of ChOx. Electron transfer is efficiently enhanced through the defects presented in the CDP-AuNP matrix.

3.6. Interferences, reproducibility and stability of cholesterol biosensors

Cholesterol is an important component in biological samples, and the selectivity of the sensor plays an important role in detection. Some common interfering substances and electrochemically active species that would possibly interfere with cholesterol determination are glucose, dopamine (DA), ascorbic acid (AA), and glycine. Fig. 7 indicates that the interferences had no effect on the detection of cholesterol, which might have resulted from the different structures and the proper working potential (0 V). In contrast, the addition of 200 μM and 100 μM cholesterol did have an obvious current response after adding these interferences into solution. Importantly, the biosensor also exhibited satisfactory reproducibility and stability after being stored in a refrigerator at 4 °C for two weeks. The stability of the sensor may be attributed to the presence of CDP-AuNP hybrid microspheres, which provided good biocompatibility and microenvironment that facilitates the bioactivity of ChOx. The CDP-AuNP hybrid microsphere as a prospective matrix displays distinguished biocompatibility and good catalytic ability. With acceptable selectivity, the proposed enzyme biosensor might potentially be used for cholesterol determination in serum samples.

The feasibility of real sample detection is one of the indicators for testing the sensor's performance. A sample of 1% human serum was applied to examine the feasibility of ChOx + CDP-AuNP + CS/

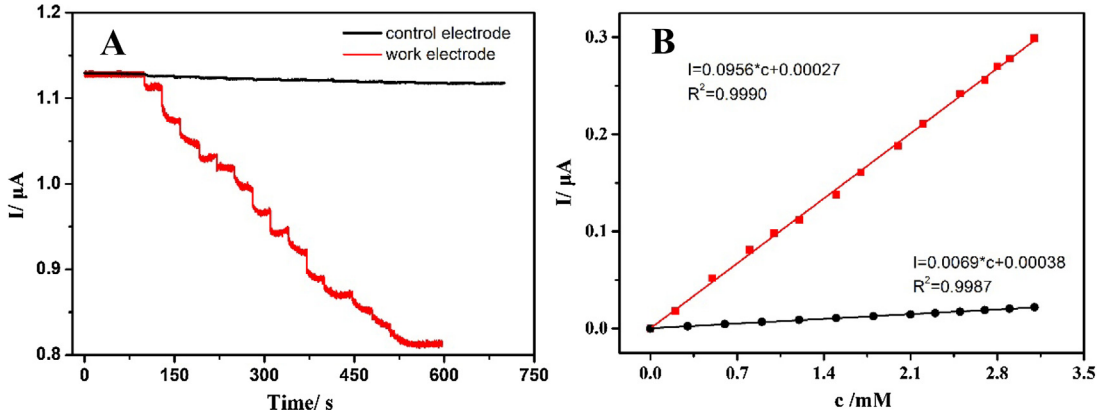

Fig. 6. (A) Amperometric responses obtained at the ChOx + CDP-AuNP + CS/PB/GCE and the controlled ChOx/CS/PB/GCE after adding a series of cholesterol from 200 μM to 3.1 mM. (B) Plot of current response vs. cholesterol.

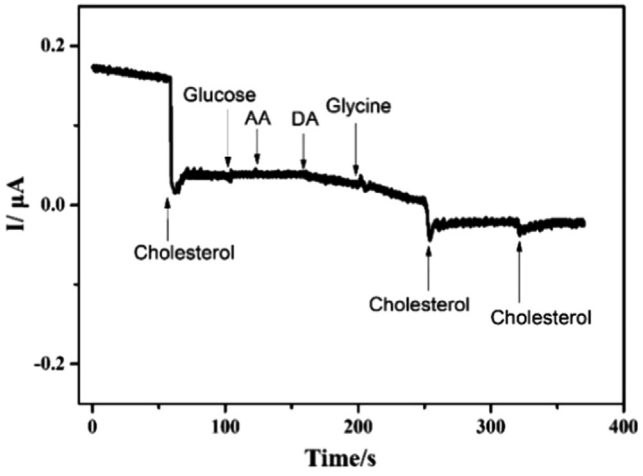

Fig. 7. Typical amperometric response of 1 mM cholesterol, 500 μM glucose, 100 μM AA, 100 μM DA, 100 μM glycine, 200 μM cholesterol and 100 μM mM cholesterol at ChOx + CDP-AuNP + CS/PB/GCE. Potential applied: 0 V vs. Ag/AgCl.

PB/GCE biosensors, as shown in Table S2. First, a cholesterol standard solution was added to the serum sample at concentrations of 1 mM, 3 mM and 5 mM. Then, the recovery was studied at the obtained biosensor. Table S2 lists the recovery received from the CDP-AuNP hybrid microsphere-modified enzyme electrodes, ranging from 96 to 98.1%. The results suggested that the developed biosensor can be used for cholesterol detection in serum. Therefore, it expanded the cholesterol biosensor's application in other biological samples.

4. Conclusions

In conclusion, cationic dipeptide-gold nanoparticle hybrid microspheres as an excellent matrix were employed to modify the enzyme electrode for cholesterol detection to achieve improved sensitivity. Hybrid microspheres on the surface of the modified electrode can retain the enzyme bioactivity and enhance the sensitivity of the biosensor by the high electrocatalytic activity of AuNPs. Importantly, the hybrid microsphere modified cholesterol oxidase electrode exhibited a current response 13 times higher than that of the controlled electrode. It also displayed more excellent sensitivity, a wider linear range, and a lower detection limit. In addition, this new cholesterol biosensor might offer great potential as an approach for biodevice detection of cholesterol in other samples, such as cell membranes.

Acknowledgements

The authors gratefully acknowledge the financial support from the National Natural Science Foundation of China (No. 21433010, 21872150, 21573248, 21872151, 21673056).

Appendix A. Supplementary material

Supplementary data to this article can be found online at https://doi.org/10.1016/j.jcis.2019.09.033.

References

[1] K. Liu, C.Q. Yuan, Q.L. Zou, Z.C. Xie, X.H. Yan, Angew. Chem. Int. Ed. 56 (2017) 7876–7880.
[2] H.C. Ma, S. Li, Y.H. Wei, L. Jiang, J.B. Li, J. Colloid Interface Sci. 514 (2018) 491–495.
[3] S.W. Huo, P.F. Duan, T.F. Jiao, Q.M. Peng, M.H. Liu, Angew. Chem. Int. Ed. 56 (2017) 12174–12178.
[4] E. Gazit, Chem. Soc. Rev. 36 (2007) 1263–1269.
[5] X.H. Yan, P.L. Zhu, J.B. Li, Chem. Soc. Rev. 39 (2010) 1877–1890.
[6] K. Tao, P. Makam, R. Aizen, E. Gazit, Science 358 (2017) eaam9756.
[7] S. Pujals, K. Tao, A. Terradellas, E. Gazit, L. Albertazzi, Chem. Commun. 53 (2017) 7294–7297.
[8] X. Han, C.X. Huang, X. Chen, Y.L. Lu, W.S. Yang, Chem. Commun. 51 (2015) 14720–14723.
[9] Q. Li, H.C. Ma, Y. Jia, J.B. Li, B.H. Zhu, Chem. Commun. 51 (2015) 7219–7221.
[10] Z.M. Yang, P.-L. Ho, G.L. Liang, K.H. Chow, Q.G. Wang, Y. Cao, Z.H. Guo, B. Xu, J. Am. Chem. Soc. 129 (2007) 266–267.
[11] S. Toledano, R.J. Williams, V. Jayawarna, R.V. Ulijn, J. Am. Chem. Soc. 128 (2006) 1070–1071.
[12] J. Ryu, C.B. Park, Adv. Mater. 20 (2008) 3754–3758.
[13] T.H. Han, J. Kim, J.S. Park, C.B. Park, H. Ihee, S.O. Kim, Adv. Mater. 19 (2007) 3924–3927.
[14] K. Ariga, Q.M. Ji, J.P. Hill, Y. Bando, M. Aono, NPG Asia Mater. 4 (2012) e17.
[15] K. Ariga, Q.M. Ji, T. Mori, M. Naito, Y. Yamauchi, H. Abe, J.P. Hill, Chem. Soc. Rev. 42 (2013) 6322–6345.
[16] X.H. Yan, Q. He, K.W. Wang, L. Duan, Y. Cui, J.B. Li, Angew. Chem. Int. Ed. 46 (2007) 2431–2434.
[17] X.H. Yan, P.L. Zhu, J.B. Fei, J.B. Li, Adv. Mater. 22 (2010) 1283–1287.
[18] Q. Li, Y. Jia, X.K. Yang, L.R. Dai, B. Das, S. Acharya, B.B. Sun, Y. Yang, X.C. Liu, K. Ariga, J.B. Li, ACS Appl. Mater. Interfaces 11 (2019) 31–36.
[19] T.T. Yuan, J.B. Fei, Y.Q. Xu, C.L. Wang, H.M. Xue, X.B. Li, G. Fytas, J.B. Li, Angew. Chem. Int. Ed. 131 (2019) 11189–11194.
[20] S.K. Li, Q.L. Zou, Y.X. Li, C.Q. Yuan, R.R. Xing, X.H. Yan, J. Am. Chem. Soc. 140 (2018) 10794–10802.
[21] M. Yemini, M. Reches, J. Rishpon, E. Gazit, Nano Lett. 5 (2005) 183–186.
[22] L. Adler-Abramovich, M. Badihi-Mossberg, E. Gazit, J. Rishpon, Small 6 (2010) 825–831.
[23] Y.T. Yaman, O. Akbal, G. Bolat, B. Bozdogan, E.B. Denkbas, S. Abaci, Biosens. Bioelectron. 104 (2018) 50–57.
[24] M. Yemini, M. Reches, E. Gazit, J. Rishpon, Anal. Chem. 77 (2005) 5155–5159.
[25] Y.F. Gong, X. Chen, Y.L. Lu, W.S. Yang, Biosens. Bioelectron. 66 (2015) 392–398.
[26] S.M. Huang, G.S. Chen, R.H. Ou, S. Qin, F.X. Wang, F. Zhu, G.F. Ouyang, Anal. Chem. 90 (2018) 8607–8615.
[27] S. Aravamudhan, A. Kumar, S. Mohapatra, S. Bhansali, Biosens. Bioelectron. 22 (2007) 2289–2294.

[28] A.N. Sekretaryova, V. Beni, M. Eriksson, A.A. Karyakin, A.P.F. Turner, M.Y. Vagin, Anal. Chem. 86 (2014) 9540–9547.
[29] N. Batra, M. Tomar, V. Gupta, Biosens. Bioelectron. 67 (2015) 263–271.
[30] S. Abraham, S. Srivastava, V. Kumar, S. Pandey, P.K. Rastogi, N.R. Nirala, S. Kashyap, S.K. Srivastava, V.N. Singh, V. Ganesan, P.S. Saxena, A. Srivastava, J. Electroanal. Chem. 757 (2015) 65–72.
[31] T.R. Lin, L.S. Zhong, H. Chen, Z.H. Li, Z.P. Song, L.Q. Guo, F.F. Fu, Microchim. Acta 184 (2017) 1233–1237.
[32] X.H. Liu, Z.H. Nan, Y. Qiu, L.C. Zheng, X.Q. Lu, Electrochim. Acta 90 (2013) 203–209.
[33] N.D. Zhou, J. Wang, T. Chen, Z.G. Yu, G.X. Li, Anal. Chem. 78 (2006) 5227–5230.
[34] H. Zhang, J.B. Fei, X.H. Yan, A.H. Wang, J.B. Li, Adv. Funct. Mater. 25 (2015) 1193–1204.
[35] N.C. Nayak, K. Shin, Nanosci. Nanotechnol. 6 (2006) 3512–3516.
[36] M. Reches, E. Gazit, Nano Lett. 4 (2004) 581–585.
[37] M. Reches, E. Gazit, Curr. Nanosci. 2 (2006) 105–111.
[38] C.Y. Song, G.P. Zhao, P.J. Zhang, N.L. Rosi, J. Am. Chem. Soc. 132 (2010) 14033–14035.
[39] J. Kim, M.J. Sadowsky, H.-G. Hur, Biomacromolecules 12 (2011) 2518–2523.
[40] A.A. Karyakin, Electroanalysis 13 (2001) 813–819.
[41] J.-C. Vidal, E. Garcia, J.-R. Castillo, Anal. Sci. 18 (2002) 537–542.
[42] H.Y. Wang, S.L. Mu, Sens. Actuators, B 56 (1999) 22–30.
[43] J.C. Vidal, E. Garcıa, J.R. Castillo, Anal. Chim. Acta 385 (1999) 213–222.
[44] Y.J. Wu, Y.D. Kong, K. Lu, M.X. Lv, Y. Ye, Y.F. Zhao, Mater. Res. Bull. 94 (2017) 278–384.
[45] A.I. Gopalan, K.-P. Lee, D. Ragupathy, Biosens. Bioelectron. 24 (2009) 2211–2217.
[46] M.K. Zachek, A. Hermans, R.M. Wightman, G.S. McCarty, J. Electroanal. Chem. 614 (2008) 113–120.